J. Sains Dasar 2022 11 (2) 118 - 125

THE CALCINATION EFFECT ON THE CRYSTALLINITY, NITROGEN CONTENT, AND PORE STRUCTURE OF NITROGEN-DOPED TITANIUM DIOXIDE

Cahyorini Kusumawardani

Departement of Chemistry, Faculty of Mathematics and Natural Science, Universitas Negeri Yogyakarta

*email : cahyorini.k@uny.ac.id

Submiited : 11 May 2022, Accepted : 14 Sepetember 2022

Abstract

Mesoporous nitrogen-doped titanium dioxide nanomaterials have been synthesized through a one-step sol gel process with dodecylamine as the pore template as well as the nitrogen source. The calcination process plays an important role in the crystallization process, determination of doped nitrogen, and pore formation. The effect of calcination temperature on the material structure was studied by calcination treatment of the as-synthesized material at several temperature variations. The resulting materials were characterized using FTIR, XRD, XPS, and N_2 gassorption analysis. The results showed that the anatase TiO_2 crystal structure began to form with calcination at 400 °C. The higher calcination temperature tends to cause the transformation of anatase crystal phase into rutile. The higher calcination temperature also affects the doped nitrogen content, where the pore-templating molecules begin to disappear at a calcination temperature and leaving a number of dopants on TiO_2. All dopants are released from TiO_2 at a calcination temperature of 600 °C. The optimum calcination temperature to form mesoporous structure was 450 °C, and the sintering occurs at a calcination temperature higher than optimum temperature indicated by the collapse of the pore structure.

Keywords: calcination, sintering effect, nitrogen-doped titanium dioxide, sintering

Introduction

Titanium dioxide (TiO_2) based materials have been intensively researched and developed for photocatalysts and photovoltaics applications since Fujishima and Honda (1972) reported the first TiO_2 photoanode in photoelectrochemical cell. TiO_2 has a fairly wide band gap energy, nontoxic, can be regenerated, easy to prepare, has high photoactivity, high surface area, high chemical and photochemical stability and does not cause secondary pollution [1]. However, the band gap energy of TiO_2 which ranges from 3 to 3.4 eV makes TiO_2 only active in the ultraviolet light region (200-400nm). This is a big problem in the utilization of TiO_2-based solar energy because only 3-5% of sunlight is emitted in the UV region [2]. Therefore, it is necessary to increase the response of TiO2 in the visible region to increase the efficiency of photocatalytic based on TiO_2.

Efforts made to shift the absorption of TiO_2 to the visible region were initially carried out by doping transition metal ions [3,4] but it was reported that metal-doped TiO_2 is thermally unstable [5] and has a tendency to form charge carrier recombination centers [4]. In addition, the high cost of ion implantation facilities makes metal doping methods difficult to develop. New intensive efforts to obtain an active TiO_2 in the visible region is the substitution of non-metallic elements such as N, C, S, P and B to the oxygen side of the TiO_2 lattice [6-9]. Among these non-metallic elements, nitrogen is reported to be the most effective dopant to improve the response of TiO_2 in the visible region [10-12] since it has similar size as oxygen and a small ionization energy of 1402.3 kJ/mol [8].

Nitrogen-doped TiO_2 provides an increased response in the visible region characterized by a shift in the absorption edge up to 600 nm [10] and a decrease in band gap energy up to 2.4 eV [12], indicated by the red shift of the absorption band edge and provide an increase in photoactivity of TiO_2 as a photocatalyst degradation reactions of colored organic compounds [11]. However, the photoactivity of TiO_2 is also highly influenced by physicochemical properties of materials such as particle size, crystallinity, and porosity [1]. TiO_2 mesoporous nanoparticles have several advantages such as high surface area and charge transfer due to easier photon induction [13]. High surface area helps exposure to effective radiation uptake and

facilitate the occurrence of photochemical reactions on the surface, while the ease of charge transfer helps the process of capture and donation of photon-induced electrons. These properties are also expected to provide benefits to the nitrogen-doped TiO_2. The photoactivity of TiO_2 is also influenced by the crystal phase of TiO_2, although the rutile phase is the most stable structure but the anatase phase is the most photoactive crystal phase [14].
The synthesis of nitrogen-doped TiO_2 has been carried out by several methods including sputtering and implantation techniques [9,15], calcination of TiO_2 with high temperatures in nitrogen-containing atmospheres [12, 16-18], and sol gel methods [19-23]. The sol gel synthesis method is one of possible method to control the level of nitrogen doping, crystallinity and porosity of nanoparticles [10].

In the synthesis of nitrogen-doped TiO_2, calcination process is being one of inportant step need to be optimized, because it determines the crystal growth and also the nitrogen-doped content. A specific calcination temperature is needed to convert the amorphous as-synthesized nitrogen-doped TiO_2 to expected anatase crystal phase and removed the precursor materials. An over high calcination temperature will lead the transformation of anatase to rutile crystal phase and the loss of high nitrogen doped. The calcined materials may be affected by the sintering process during the calcination which will collapted the pore. This article reported the effect of calcination temperature towards crystallinity, nitrogen content, and sintering effect, of nitrogen-doped TiO_2.

Methods

Materials

Titanium tetra isopropoxide (TTIP) 97% was purchased from Aldrich, dodecylamine (DDA) 98%, was obtained from Fluka, while ethanol absolute and acetic acid glacial were purchased from Merck. All materials were used as received without further purification.

Synthesis of Nitrogen-doped TiO_2

The synthesis of nitrogen-doped TiO_2 was done following previous developed procedures [6] by refluxing the mixture of dodecylamine and TTIP ethanolic solution in the pH of 5. The solution was the hydrolized by the dropwise addition of 25 mL deionized water under vigorous stirring and continued stirring for 24 hours, continued by aging process of 72 hours. The resulting yellowish precipitates were filtered and washed using distilled water and ethanol (1/1 V/V). The powder was calcined at varied temperature from 100-800 °C at a heating rate of 2 °C /min in an air atmosphere for 4 hours.

Characterization

The crystal structure of the resulted N-doped TiO2 powder was characterized using an X-ray Powder Diffractometer (Shimadzu, X-6000) with Cu Kα radiation (λ = 0.15406 nm). The specific surface area was examined by standard BET equipment (Quantochrome Autosorb-2) and Barret-Joyner-Halenda (BJH) was used to determine the pore size distribution. The elemental analysis was done using X-ray Photoelectron Spectroscopy analysis (Thermo-advantage 5200W).

Results and Discussions

The effect of calcination treatment on the character of nitrogen-doped TiO_2 was studied by calcining the as synthesized material for 4 hours at several temperature variations with a temperature increase rate of 2 °C /min. Changes in functional groups that occur during the calcination process were characterized by FTIR, as shown in Figure 1. Based on the FTIR spectra, it can be seen that the calcination treatment was effective enough to remove the dodecylamine molecule as the pore template and nitrogen source, which was characterized by the disappearance of residual organic groups of the dodecylamine molecule. Organic groups began to escape from N-doped TiO_2 after calcination at 300 °C indicated by the disappearance of C-H vibrational bands in the region around 1350 cm^{-1} and 2800-3000 cm^{-1}. O-H and N-H vibrational bands that coincide in the area around 3200-3500 cm^{-1} no longer appeared in the spectra of the material calcined at 450 °C, indicating that the dodecylamine molecules have completely disappeared from the synthesized material. However, there are still peaks in the ~2350 cm^{-1} and ~1650 cm^{-1} regions that indicate the presence of carbon and nitrogen species in TiO_2 [10].

The crystal growth from amorphous structure into a crystalline structure (crystallization process) leaded by the calcination process was also confirmed by FTIR spectra. The presence of anatase TiO_2 crystal structure is indicated by the wide and strong peak in the region of 300-700 cm^{-1} as also reported by Gonzales *et al* [24]. The sharp peak in the region of 360 cm^{-1} shows the characteristics of anatase Ti-O structure which is getting sharper with

increasing crystallinity as also reported by Sankapal, *et al*. [25].

The releasing process of dodecylamine molecules in the as-synthesized N-doped TiO_2 was then focused out by FTIR analysis of the material calcined at 450 °C and dodecylamine as a reference (Figure 2). It indicates the presence of organic precursor functional groups adsorbed on the surface of as- synthesized material with the presence of C-H stretching vibrational bands between 1800-1300 cm^{-1} and 2800-3500 cm^{-1}. The -NH_2 group of dodecylamine appeared in the area around 1600-1700 cm^{-1} and 3000-3500 cm^{-1}. The region below 1000 cm^{-1} is characteristic of Ti-O-Ti framework vibrations. These organic groups of dodecylamine disappeared in the N-doped TiO_2 material after calcination at 450 °C. There is still shows a band peak in the ~1650 cm^{-1} region which indicates the N-H vibrational band, revealing the presence of nitrogen doping or adsorbed on TiO_2 as also reported by many researchers [10,12,26-29].

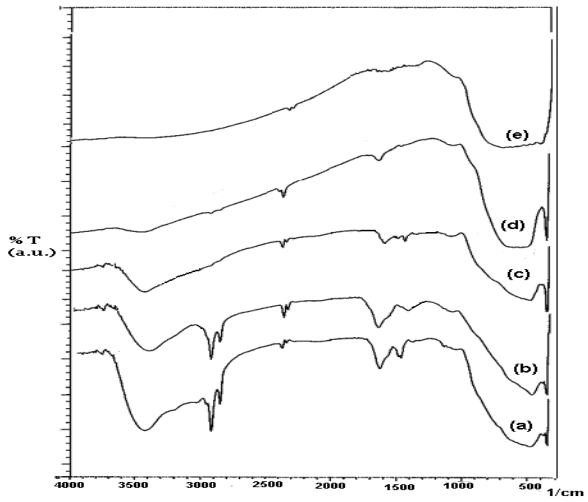

Figure 1. FTIR spectra of nitrogen-doped TiO_2 :(a).as-synthesized ; (b) calcined at (b) 200; (c) 300; (d) 450 dan (e) 600 °C

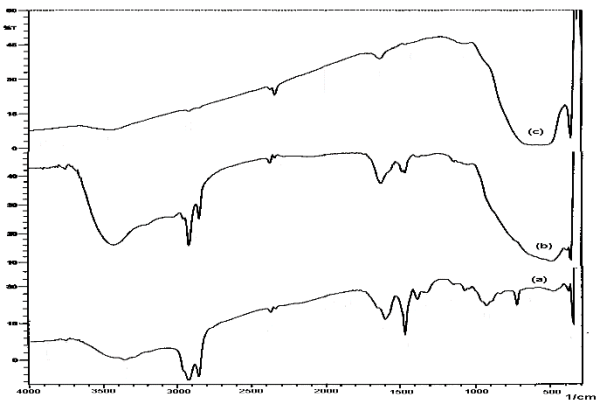

Figure 2. FTIR spectra of (a) dodecylamine; (b) synthesized N-doped TiO_2 powder and (c) N-TiO2 after calcination at 450 ^oC

XRD analysis of the calcined material at various temperatures presented in Figure 3, which shows that calcination treatment greatly affects the formation of N-doped TiO_2 crystals. XRD spectra confirm that N-doped TiO_2 is amorphous even after calcined at temperatures <400 ^oC. The anatase crystal phase began to form after calcination at 400 ^oC as indicated by the diffractogram peaks at 2θ = 25.30; 38.1; 48.2; 53.9 and 55.1^o according to the standard XRD pattern (JCPDS No. 21-1272). Anatase to rutile transformation began to occur when calcination was carried out at a temperature of 500 °C as indicated by the appearance of diffractogram peaks at 2θ = 27.28; 36.1; 41.3; 44.2; and 55.5^o; which represents the characteristics of the rutile phase TiO_2 tetragonal crystal (JCPDS No. 21-1276).

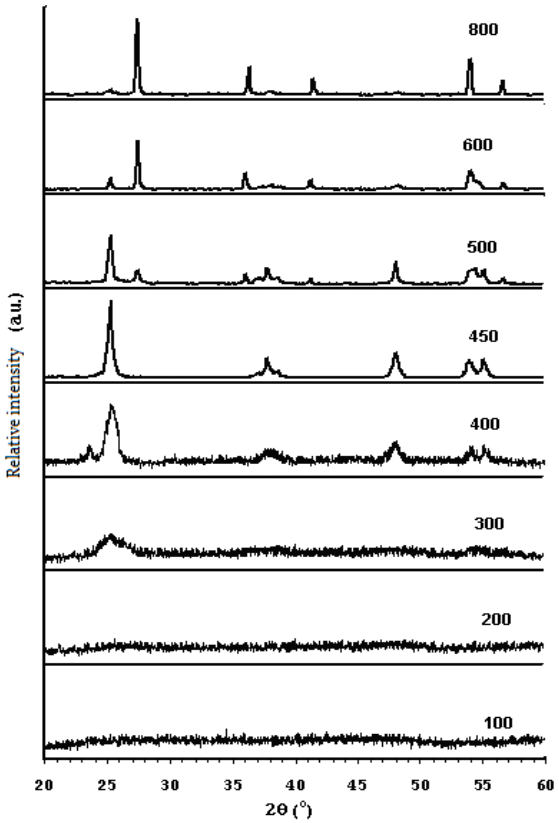

Figure 3. XRD diffractogram of N-doped TiO_2 after calcination treatment for 4 hours at various temperatures

The calcination process not only aims to remove template molecules, but is also intended as a crystal formation process. Calcination at 400 - 450 °C produces anatase crystal structure. This is in

accordance with the data reported by Vinodgopal *et al.* [30] and Burda *et al.* [31] which state that the anatase crystal phase is formed from synthesis at low temperatures followed by calcination at 400-500 °C; however, in this study the rutile crystal phase was formed at 500 °C. Calcination at a temperature higher than 500 °C causing the higher transformation of the anatase phase to the rutile phase, and also lead to the loss of nitrogen dopants from TiO_2 nanoparticles.

The change in the ratio of anatase phase to rutile phase due to calcination treatment at different temperatures is shown in Figure 4. Calcination treatment at temperatures >450 °C greatly affects the ratio of anatase to rutile, namely the higher the calcination temperature causes a decrease in the ratio of anatase to rutile. Calcination at 500 °C causes ~20% of the anatase structure to change into a rutile structure. The anatase to rutile ratio drops dramatically when calcined at 600 °C with ~85% of the anatase phase transforming into the rutile phase. The anatase phase is almost completely transformed into rutile when calcined at 800 °C. This means that calcination at temperatures up to 450 °C plays a role in the crystal growth process, while calcination at high temperatures (>450 °C) plays a role in the process of N-doped TiO_2 crystal phase transformation.

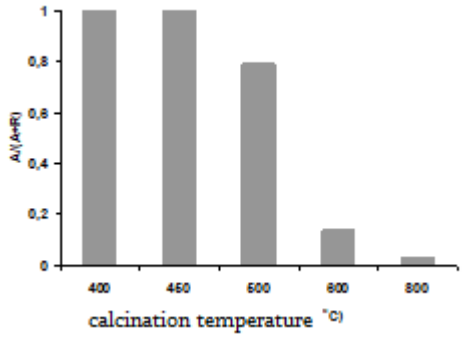

Figure 4. Anatase to rutile phase ratio (A/(A+R)) at various calcination temperatures

The crystal size of the N-doped TiO_2 sample calculated based on the peak field (101) (antase phase) and peak field (110) (rutile phase) on the XRD diffractogram according to the Scherrer equation solution as shown in Figure 5, shows that the crystal size (grain size) increases with increasing calcination temperature. The growth of crystal size can be viewed from the growth of crystal particles (particle growth) relative to the growth of crystal nucleation (particle nucleation). Increasing temperature causes an increase in particle growth rate and nucleation growth rate. In this study, for all temperature variations, the rate of formation of crystal nuclei is in line with the rate of particle growth, namely an increase in crystal size that is linear to the increase in calcination temperature.

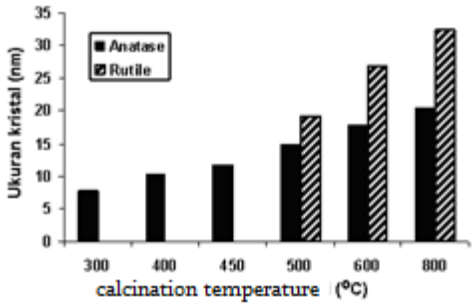

Figure 5. Crystal size of N-doped TiO_2 samples at various calcination temperatures

The influence of calcination to the nitrogen-doped content was also studied using XPS analysis and the results shown in Figure 6. XPS spectra of N-doped TiO_2 calcined at 200, 450 and 600 °C, showed that the increase in calcination temperature resulted in a decrease in the intensity of carbon and nitrogen peaks. This means that calcination treatment is effective for removing organic residues derived from dodecylamine molecules in the synthesized N-doped TiO_2 material. The high intensity of the C_{1s} and N_{1s} peaks in the spectrum of the calcined sample at 200 °C indicates the presence of organic groups in the sample. This is in accordance with the results of FTIR analysis, where the organic groups disappear after heating at temperatures >450 °C. The XPS spectrum of N-doped TiO_2 after calcination at 450 °C still shows the presence of nitrogen and carbon band peaks in the sample, but the peaks disappear in the spectrum of the sample calcined at 600 °C which means that all nitrogen and carbon are released when heating at high temperatures (>470 °C).

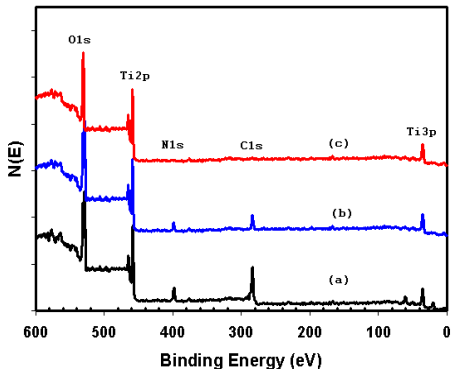

Figure 6. XPS spectra of N-doped TiO_2 calcined at (a) 200; (b) 450 and (c) 600 °C

The change in nitrogen content due to calcination treatment was analyzed through the N1s binding energy spectra (Figure 7). The release of nitrogen due to the calcination process can be confirmed by the N_{1s} binding energy spectra. In the N_{1s} spectrum of the 200°C calcined sample, there is one broad band peak centered at 399.4 eV. The existence of the band peak comes from dodecylamine nitrogen organic groups that have not been completely released at a calcination temperature of 200 °C based on FTIR. According to Asahi *et.al.* [14], the existence of a band peak in the ~400 eV region indicates the presence of nitrogen doping on TiO_2 which can take the form of adsorbed N_2, NH_x, or NO_x and also N^- (γ-N) species that are bound substitutionally to the TiO_2 lattice.

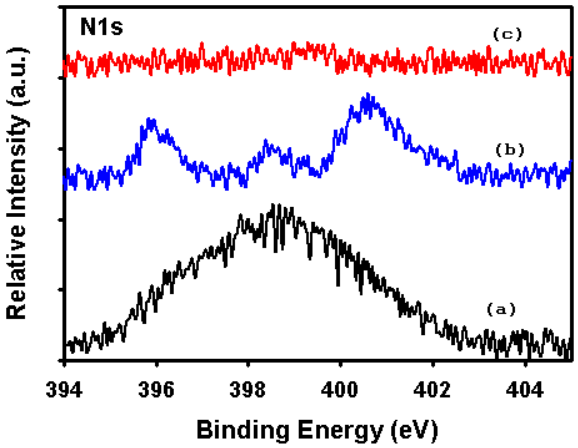

Figure 7. N_{1s} XPS spectra of N-doped TiO_2 calcined at (a) 200; (b) 450 and (c) 600 °C

The broad band peak is separated into three distinct band peaks in the spectra of the sample calcined at 450 °C. Most researchers interpret the two higher energy peaks as emissivated N_2, adsorbed NH_x or NO_x, while the band peak at 396 eV signifies N^- (γ-N) species substitutionally bound to the N-doped TiO_2 lattice [12,32]. Likewise with Asahi *et al.* [14] which marks the band peak at 396 eV as a substitutional N replacing O on the TiO_2 lattice and band peaks at 400 and 402 eV as emissivated N_2 molecules. Gopinath et al. [33] also concluded that the band peaks in the region above 400 eV are associated with oxidized nitrogen such as N-O-Ti-O or O-N-Ti-O, while the band peaks in the 396-397 eV region as substitutional N doping. The negative charge contribution of substitutional nitrogen species bound to positively charged Ti lowers the binding energy of N- species.

A different N 1s spectrum analysis was reported by Chen and Burda [10], where a broad band peak between 397.4-403.7 eV centered at 401.3 eV was characterized as oxynitride formation by substitutional N doping. Chen and Burda did not report any other species that may exist on TiO_2 because the interpretation of the N 1s binding energy peak was considered as a single band peak. The separation of a single band peak from the material calcined at 200 °C into three band peaks at 450 °C indicates a decrease in nitrogen doping content because the decrease in peak intensity indicates the presence of each species. The three band peaks disappeared at a calcination temperature of 600 °C which indicates the release of nitrogen from TiO_2. The disappearance of the N1s binding energy peak at 600 °C calcination indicates that the nitrogen content of TiO2¬ becomes unobserved (<1%).

The Ti_{2p} binding energy spectra (Figure 8) also confirm the loss of nitrogen from the N-doped TiO_2 sample at a calcination temperature of 600 oC. All $2p^{3/2}$ band energy peaks of the three spectra are located in the region between pure TiO_2 (459.1 eV) and pure TiN (455.3 eV). The binding energy of Ti $2p^{3/2}$ N-TiO2 calcined at 600 °C is centered at 459 eV, while the other two spectra are centered in the lower region of ~458 eV. This indicates that the Ti center ion is very sensitive to the electronic environment of the atoms around it, by adding negatively charged N into the TiO_2 matrix causes the binding energy of Ti to be lower. Reducing the nitrogen doping content, causes the binding energy of Ti to be higher. This also indicates that increasing the calcination temperature can cause the release of nitrogen doping which is characterized by a shift in the binding energy peak of Ti $2p^{3/2}$ towards the peak of pure TiO_2.

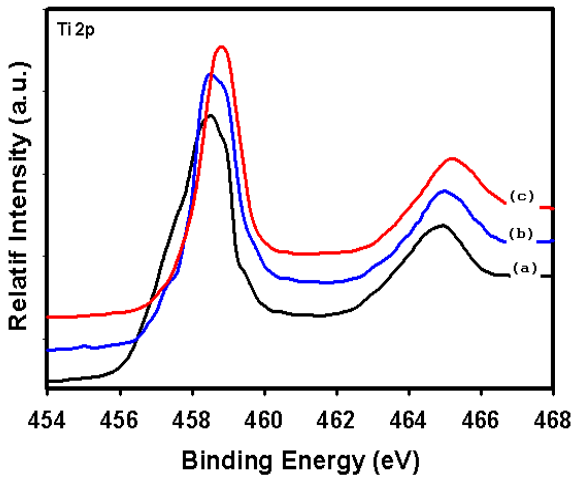

Figure 7. Ti_{2p} XPS spectra of N-doped TiO_2 calcined at (a) 200; (b) 450 and (c) 600 °C

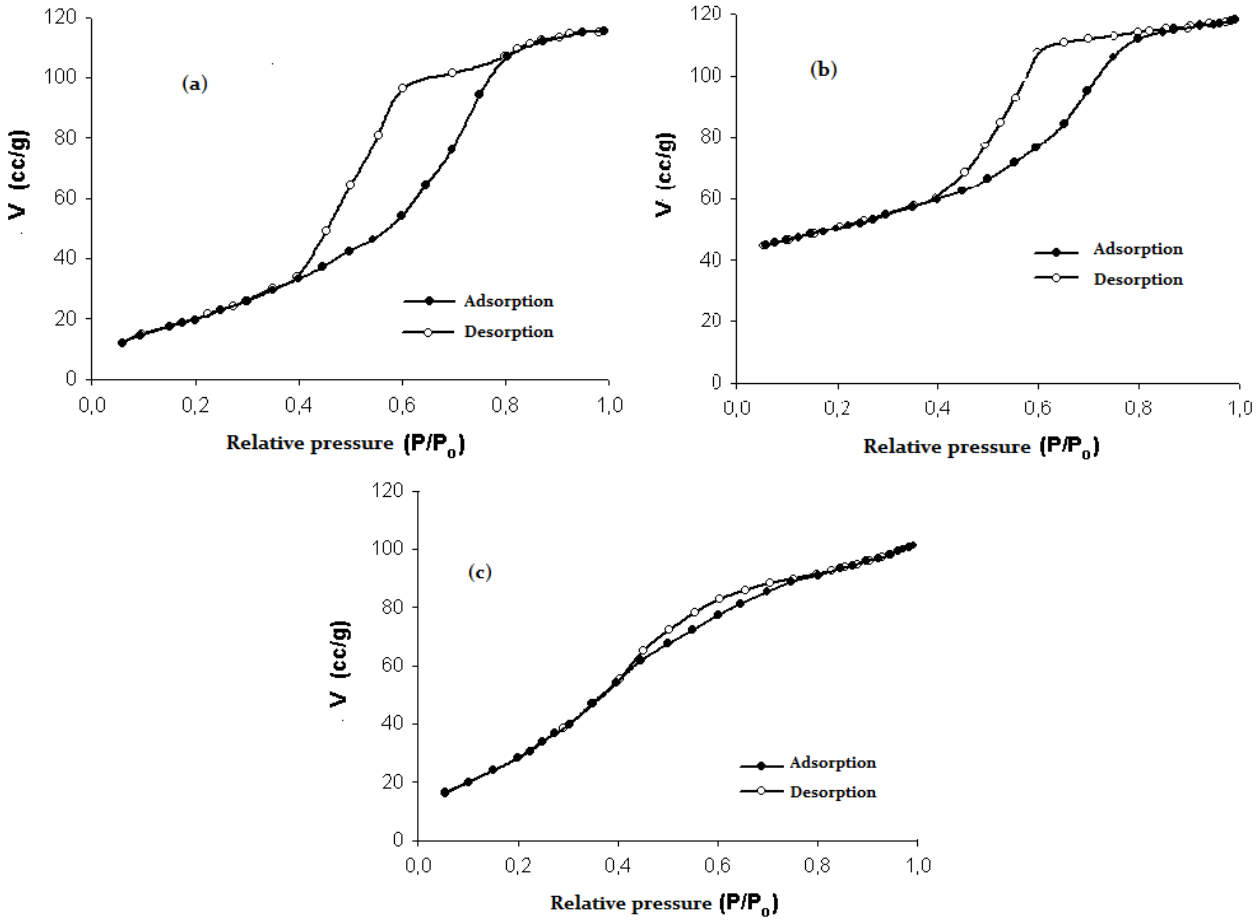

Figure 8. N_2 adsiorption-desorption isotherm of N-doped TiO_2 calcined at (a) 200; (b) 450 and (c) 600 °C

The effect of calcination to the porosity was studied using N_2 adsorption desorption analysis and the results showed in Figure 8. It revealed that the calcination temperature is highly affect the porosity of materials. The calcination process facilitates the formation of pore by releasing the pore template. However the higher and the longer calcination process tend to the sintering effect which lead to the pore collapse since the material moves to the contact points between particles and fills in the open space. According to the crystallinity, nitrogen-doped content, and porosity, calcination temperature of 450 ^{O}C is being an optimum temperature to result in nitrogen-doped TiO_2 mesopore nanoparticles.

Conclusion

Mesoporous nitrogen-doped titanium dioxide nanomaterials have been successfully synthesized through a one-step sol gel process. The calcination process plays an important role in the crystallization process, determination of doped nitrogen, and pore formation. The results showed that the anatase TiO_2 crystal structure began to form with calcination at 400 °C. The higher calcination temperature tends to cause the transformation of anatase crystal phase into rutile. The higher calcination temperature also affects the doped nitrogen content, where the pore-templating molecules begin to disappear at a calcination temperature of 400 °C leaving a number of dopants on TiO_2. All dopants are released from TiO_2 at a calcination temperature of 600 ^{O}C. the formation of mesopore structure begins at a calcination temperature of 200 °C and optimum at a temperature of 450 °C. sintering process occurs at a calcination temperature of 600 °C indicated by the collapse of the pore structure.

Acknowledgement

Financial support from Indonesian Government granted by Universitas Negeri Yogyakarta through Program Percepatan Guru Besar Tahun 2020 is gratefully acknowledged.

References

[1] Kusumawardani C., Suwardi, Kartini I. and Narsito. (2012), Synthesis and Characterization of N-doped TiO_2 Photocatalyst, *Asian J. Chem.*, 24, 1, , 255–256

[2] Foo C., Li Y., Lebedev K., Chen T., Day S., Tang C. & Tsang E. (2021), Characterisation of oxygen defects and nitrogen impurities in TiO_2 photocatalysts using variable-temperature X-ray powder diffraction. *Nat Commun.*, 12, 661. https://doi.org/10.1038/s41467-021-20977-z

[3] Ibrahim N.S., Leaw W.L., Mohamad D., Alias S.H., Nur H. (2020), A critical review of metal-doped TiO_2 and its structure–physical properties–photocatalytic activity relationship in hydrogen production, *International Journal of Hydrogen Energy*, 45, 53, 28553-28565. https://doi.org/10.1016/j.ijhydene.2020.07.233

[4] Basavarajappa P.S, Patil S.B., Ganganagappa N., Keddy K.R., Raghu A.V., Reddy C.V. (2020), Recent progress in metal-doped TiO_2, non-metal doped/codoped TiO_2 and TiO_2 nanostructured hybrids for enhanced photocatalysis, *International Journal of Hydrogen* Energy, 45, 13, 7764-7778. https://doi.org/10.1016/j.ijhydene.2019.07.241

[5] Choi W., Termin A. and Hoffmann M.R. (1994), Effects of metal-ion dopants on the photocatalytic activity of quantum-sized TiO_2 particles, *Angew. Chem.* 106, 1148–1149

[6] Kusumawardani, C. (2021), The Pore Formation anda Doping Process on the Synthesis of Nitrogen-doped Titania Through Sol-gel Method, Rasayan. J. Chem., 15, 1, 549-556. http://dx.doi.org/10.31788/RJC.2022.1516674

[7] Kim T.H., Go G-M., Cho H-B., Song Y., Li C-G., Choa Y-H. (2018), A Novel Synthetic Method for N Doped TiO_2 Nanoparticles Through Plasma-Assisted Electrolysis and Photocatalytic Activity in the Visible Region, *Front. Chem.*, 6, 458. https://doi.org/10.3389/fchem.2018.00458

[8] Shehata M.A., Shama S.A., Mahmoud S.A., Doheim M.M. (2016), Preparation and Characterization of Various Interstitial N-Doped TiO_2 Catalysts from Different Nitrogen Dopants for the Treatment of Polluted Water, *Chemistry and Materials Research*, 8, 6, 45-55.

[9] Khan T.T., Bari R.,Kang H-J., Lee T-G., Park J-W., Hwang H.J., Hossain S.M., Mun J.S., Suzuki N., Fujishima A., Kim J-H., Shon H.K. and Jun Y.S. (2021), Synthesis of N-Doped TiO_2 for Efficient Photocatalytic Degradation of Atmospheric NO_x, *Catalysts*, 11, 1, 109. https://doi.org/10.3390/catal11010109

[10] Chen X. and Burda C. (2004), Photoelectron Spectroscopic Investigation of Nitrogen-Doped Titania Nanoparticles, *J. Phys. Chem. B*, 108 (40), 15446-15449

[11] Irie H., Watanabe Y and Hashimoto K. (2003), Nitrogen-Concentration Dependence on Photocatalytic Activity of $TiO_{2-x}N_x$ Powders, *J. Phys. Chem. B*, 107 (23), 5483-5486

[12] Nosaka, Y. Matsushita, M. Nishino, J. Nosaka, A.Y., (2019), Nitrogen-doped titanium dioxide photocatalysts for visible response prepared by using organic compounds, *Sci. Tech. Adv. Mater.*, 6, 143-148

[13] Natarajan T.S., Mozhiarasi V. and Tayade R.J. (2021), Nitrogen Doped Titanium Dioxide (N-TiO_2): Synopsis of Synthesis Methodologies, Doping Mechanisms, Property Evaluation and Visible Light Photocatalytic Applications, *Photochem*, 1, 3, 371-410. https://doi.org/10.3390/photochem1030024

[14] Asahi R., Morikawa T., Ohwaki T., Aoki K. And Taga Y., 2001, Visible-Light Photocatalysis in Nitrogen-Doped Titania,

Science, 293, 269-271

[15] Bakar S.A. and Ribeiro C. (2016), Nitrogen-doped titanium dioxide: An overview of material design and dimensionality effect over modern applications, *Journal of Photochemistry and Photobiology C: Photochemistry Reviews*, 27, 1-29. https://doi.org/10.1016/j.jphotochemrev.2016.05.001

[16] Nakamura R., Tanaka T., Nakato Y. (2004), Mechanism for Visible Light Responses in Anodic Photocurrents at N-Doped TiO_2 Film Electrodes, *J. Phys. Chem. B*, 108 (30), 10617-10620

[17] Diwald O., Thompson T.L., Goralski E. G., Walck S. D. & Yates J.T. Jr. (2004), The effect of nitrogen ion implantation of the photoactivity of TiO2 rutile single crystals. *J. Phys. Chem. B*, 108, 52-57

[18] Cheng X., Yu X., Xing Z., Yang L. (2016), Synthesis and characterization of N-doped TiO2 and its enhanced visible-light photocatalytic activity, Arabian J. Chem., 9, 2, S1706-S1711. https://doi.org/10.1016/j.arabjc.2012.04.052

[19] Qiu and Burda, (2007), Chemically Synthsized Nitrogen-doped Metal Oxide nanoparticles, *Chem. Phys*, 339, 1 – 10

[20] Sakthivel S., Janczarek M., Kisch H. (2004), Visible light activity and photoelectrochemical properties of nitrogen-doped TiO_2, *J. Phys. Chem. B*, 108, 19384-19387

[21] Tachikawa T., Takai Y., Tojo S., Fujitsuka M., Irie H., Hashimoto K., Majima T. (2006) Visible Light-Induced Degradation of Ethylene Glycol on Nitrogen-Doped TiO_2 Powders, *J. Phys. Chem. B*, 110, 13158-13165

[22] Valentin C.D., Finazzi E., Pacchioni G., Selloni A., Livraghi S., Paganini M.C. and Giamello E., (2005), N-doped TiO_2: Theory and Experiment, *Chem. Phys.*, 339, 44-56

[23] Kusumawardani, C., Sugiyarto K.H., Prodjosantoso A.K. (2021), The influence of ph on the nitrogen-doped tio2 structure and its photocatalytic activity on methylene blue degradation, *Molekul*, 16, 3, 270-279. http://dx.doi.org/10.20884/1.jm.2021.16.3.804

[24] Gonzales R.J. (1996), *Raman, Infra Red, X-Ray and EELS Studies of Nanophase Titania*, Dissertation, Faculty of the Virginia Polytechnic Institute and State University, Blacksburg

[25] Sankapal B.R., Lux-Steiner,M.C. and Ennaoui, A. (2005), Synthesis and Characterization of Anatase TiO_2 Thin Films, *Appl. Surf. Sci.*, 239, 165-170

[26] Giles E. Eperon, Severin N. Habisreutinger, Tomas Leijtens, Bardo J. Bruijnaers, Jacobus J. van Franeker, Dane W. deQuilettes, Sandeep Pathak, Rebecca J. Sutton, Giulia Grancini, David S. Ginger, Rene A. J. Janssen, Annamaria Petrozza, and Henry J. Snaith, The Importance of Moisture in Hybrid Lead Halide Perovskite Thin Film Fabrication, *ACS Nano*, 9, 9, (2015), 9380–9393, https://doi.org/10.1021/acsnano.5b03626

[27] Sarah Wozny, Mengjin Yang, Alexandre M. Nardes, Candy C. Mercado, Suzanne Ferrere, Matthew O. Reese, Weilie Zhou, and Kai Zhu, Controlled Humidity Study on the Formation of Higher Efficiency Formamidinium Lead Triiodide-Based Solar Cells, *Chemistry Materials*, 27, 13, (2015), 4814–4820, https://doi.org/10.1021/acs.chemmater.5b01691

[28] Vitiello R., Macak J., Ghicov A., Tsuchiya H., Dick L. and Schmuki P., (2016), N-Doping of anodic TiO_2 nanotubes using heat treatment in ammonia. *Electrochem. Commun.*, 8, 544-548

[29] Kusumawardani C. andIkhsan J. (2022), The Synthesis of Methylammonium Lead Iodide on Mesopore TiO_2 Thin Film Applying Ostwald Ripening Process Under Ambient Condition, *Rasayan Journal of Chemistry*, 15, 3, 1678–1685, https://doi.org/10.31788/RJC.2022.1536890

[30] Vinodgopal K., Hua X., Dahlgren R.B., Lappin A.G., Patterson L.K. and Kamat P.V. (2020), Photochemistry of $Ru(bpy)_2(dcpy)^{2+}$ on Al_2O_3 and TiO_2 surface. An Insight into the Mechanism of photosensitization, *J. Phys. Chem.*, 99, 10883-10889

[31] Burda C., Samia A.C.S., Hathcock D., Huang H. and Yang S. (2004), N-Doped TiO_2 Nanotube With Visible Light Activity, *J. Am. Chem. Soc.*, 124(42), 12400-12401

[32] Lindgren T., Mwabora J.M., Avendano E., Jonsson J., Hoel A., Granqvist C., Lindquist S. (2003), Photoelectrochemical and Optical Properties of Nitrogen Doped Titanium Dioxide Films Prepared by Reactive DC Magnetron Sputtering, *J. Phys. Chem. B*, 107 (24), 5709-5716

[33] Gopinath C.S. (2006), Photoelectron Spectroscopic Investigation of Nitrogen-Doped Titania Nanoparticles, *J. Phys. Chem. B*, 110, 7079-7082